Rapid climate transitions in a coupled ocean–atmosphere model

Stefan Rahmstorf

Institut für Meereskunde, Düsternbrooker Weg 20, 24105 Kiel, Germany

RECENT geochemical data[1,2] have challenged the view that rapid climate fluctuations in the North Atlantic at the end of the last glacial were caused by the thermohaline circulation of the ocean being switched 'on' or 'off'. Instead, these data suggest that the circulation pattern must have switched between a warm, deep mode and a cold, shallow mode, probably associated with different sites of deep convection[3]. Here I present simulations with a three-dimensional ocean model, coupled to an idealized atmosphere, which show this kind of transition. The mechanism for the transition is a rearrangement of convection in the North Atlantic, triggered by a brief freshwater pulse. This results in a drop in sea surface temperature in the North Atlantic by up to 5 °C within less than 10 years. The rate of North Atlantic Deep Water (NADW) formation is the same in the cold climate as in the warm climate, but NADW sinks to intermediate depths only, while Antarctic Bottom Water pushes north to fill the entire abyssal Atlantic.

Palaeoclimate studies show that rapid climate changes in the North Atlantic region are correlated with changes in NADW flow[2,4,5]. It is widely believed that because the NADW thermohaline 'conveyor belt' has the capacity to transport large amounts of heat towards the northern North Atlantic (at present $\sim 0.5 \times 10^{15}$ W, leading to a warming of 4 °C compared with the northern North Pacific[6,7]), some of the climate changes visible in the palaeoclimate records are caused by variations in the conveyor belt. This idea is supported by modelling studies, which have demonstrated that the conveyor belt is a self-sustaining circulation which can collapse when disturbed, and which can have multiple steady states[8–10]. Within this picture, a large freshwater perturbation, like the sudden inflow of melt water just before the Younger Dryas event, could have triggered the complete collapse of the conveyor belt, leading to a rapid cooling of the North Atlantic by several degrees within about a decade.

More recent data do not fit this interpretation, however[1,2]. They show that even during cold periods the conveyor did not stop; NADW flow continued at similar intensity. However, the sites of deep convection appear to have shifted, and NADW flow was probably shallower than during warm periods. Previous model studies of the conveyor are unable to explain these results.

The experiments reported here, using the Geophysical Fluid Dynamics Laboratory (GFDL) ocean circulation model, are consistent with the new data. I have used an idealized configuration with two square ocean basins of equal size, representing Pacific and Atlantic, (as in ref. 10; see Fig. 3*a*). The model was driven by a simple zonal-mean wind stress. The freshwater flux at the ocean surface was diagnosed from a spin-up experiment, zonally averaged and then held fixed. The traditional 'restoring' boundary condition[11] on temperature, used in previous ocean model studies, was replaced by

$$Q = \gamma(T^* - T_O) - \mu\nabla^2(T^* - T_O) \qquad (1)$$

This equation derives from an energy balance model of the atmosphere with diffusive horizontal transport of temperature anomalies[12]. Q is the heat flux at the ocean surface, T_O the ocean surface temperature, γ a radiative relaxation constant ($3\ \mathrm{W\,m^{-2}\,K^{-1}}$), μ a constant related to atmospheric heat diffusion ($8 \times 10^{13}\ \mathrm{W\,K^{-1}}$), and T^* defines a climate without oceanic heat transport, around which equation (1) is linearized. T^* was prescribed as a cosine function of latitude, symmetric in both hemispheres. In contrast to classical restoring, where the atmospheric temperature is assumed fixed and the heat flux from the ocean disappears into an 'infinite sink' atmosphere, equation (1) represents a closed heat budget where heat leaving the ocean can only be lost to space through long-wavelength radiation (first term) or redistributed laterally within the atmosphere by turbulent diffusion (second term). Atmospheric temperature is a diagnostic variable in this model; from equation (1) it has already been eliminated by inserting the atmospheric heat budget equation. Equation (1) is thus suitable for climate studies and allows the prediction of changes in surface temperature resulting from ocean circulation changes.

A conveyor-belt circulation was spun up in the usual way[10,12]. The resulting model equilibrium has a realistic temperature contrast (not shown here) between North Atlantic and North Pacific due to the conveyor's heat transport and in spite of the zonally uniform forcing. Another realistic feature is the appearance of an Antarctic Bottom Water (AABW) cell underneath the NADW cell in the Atlantic (Fig. 1*a*), caused by colder temperatures in the Southern Ocean compared to the northern convection region. Previous ocean models had to prescribe these colder temperatures in the forcing field in order to get AABW; here they are a natural consequence of the conveyor circulation.

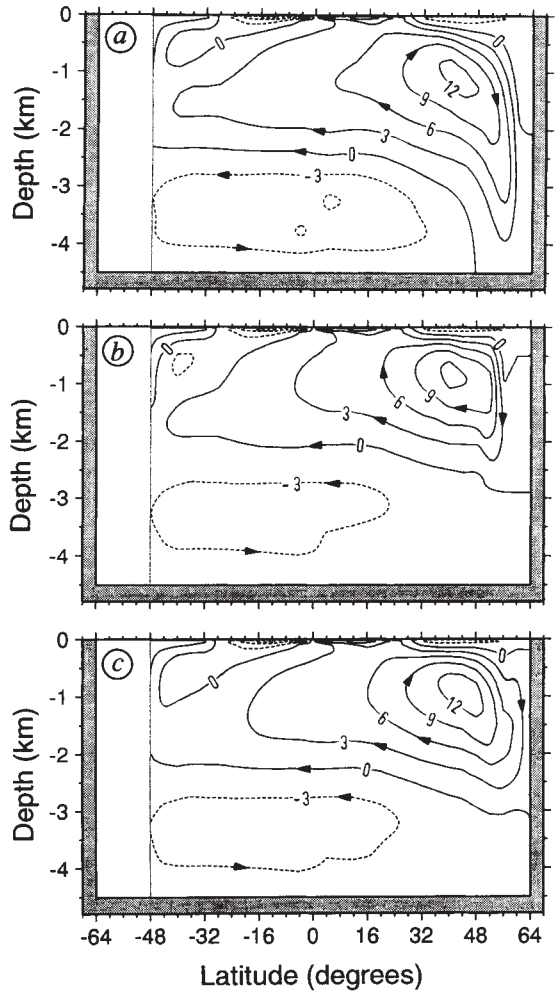

FIG. 1 Zonally integrated meridional mass transport in $10^6\ \mathrm{m^3\,s^{-1}}$ in the Atlantic model basin: *a*, for the spin-up conveyor state; *b*, for the equilibrium reached after the first freshwater perturbation; *c*, for the equilibrium after the second perturbation. These three coupled equilibria exist under the same forcing. Note that in *b* and *c* the North Atlantic Deep Water (NADW) cell does not reach down to the bottom of the North Atlantic.

To test the stability of this state, a strong freshwater pulse was then added to the North Atlantic north of 56° N for 4 years. Time series of important model parameters during this experiment are shown in Fig. 2. The freshwater surge temporarily interrupts convection and slows the conveyor, but 20 years after the end of the perturbation deep water formation has recovered to its original rate. Temperature in the northern North Atlantic region has changed permanently and drastically, however, dropping by an average 2.6 °C north of 48° N, and 3 °C north of 56° N. Average salinity north of 56° N has dropped by 1‰. At the same time, NADW flow has become shallower, while AABW now penetrates northward in the abyssal Atlantic up to the northern wall (Fig. 1*b*); similar northward AABW incursions are also found in palaeoclimate data[13]. The pattern of sea surface temperature change is shown in Fig. 3*a*. Cooling occurs in the whole North Atlantic with a maximum in high latitudes, particularly in the west where the northward flowing boundary current is weakened. These features resemble the pattern of observed interdecadal variability during this century[14]. The remainder of the ocean surface warms, most notably in the South Atlantic, where the increase exceeds 0.5 °C in some regions.

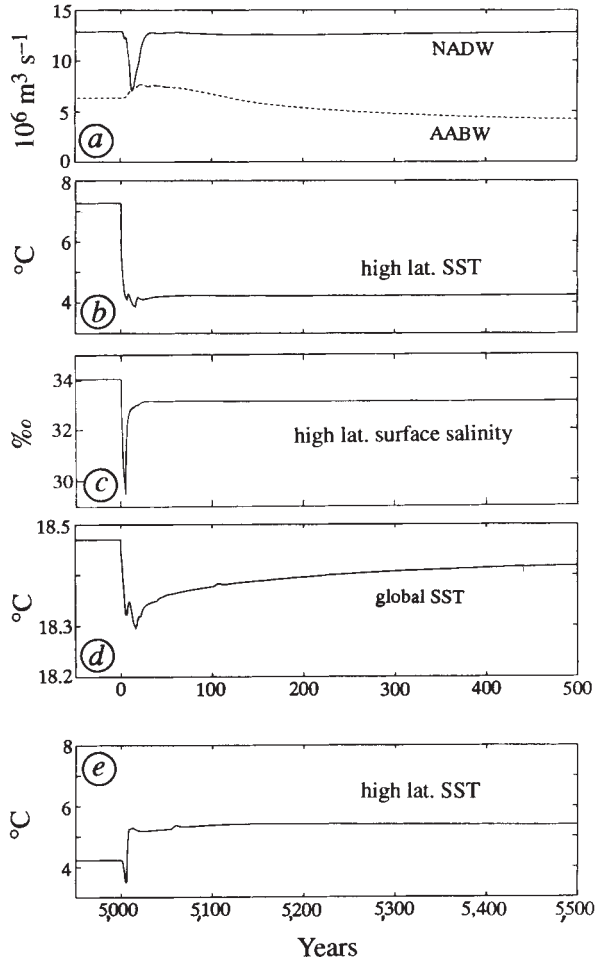

FIG. 2 Time series of model parameters during and after the freshwater perturbation (starting at $t = 0$ for 4 years). *a*, Strength of the NADW cell (solid) and the Antarctic Bottom Water (AABW) cell (dashed) in the Atlantic basin. *b*, Mean sea surface temperature (SST) in the Atlantic north of 56° N (high lat.). *c*, Mean sea surface salinity in the Atlantic north of 56° N. *d*, Mean SST of the entire model domain. *e*, Same as *b*, but for the second freshwater perturbation (at $t = 5{,}000$ yr). Note that even the 'global' SST (*d*) is affected by the perturbation, due to transient heat uptake by the deep ocean, although its equilibrium value is fixed by equation (1) (see text).

The model was integrated for 5,000 years after the perturbation to reach equilibrium, and then the same freshwater perturbation was applied once more. Again a permanent transition to a different circulation state was triggered, this time accompanied by moderate warming in the North Atlantic region (Figs 1*c*, 2*e*). The deep-water formation rate in all three equilibria is remarkably similar, probably due to a negative temperature feedback discussed by Rahmstorf[15].

Unlike the 'on/off' transition found in previous models, caused by the advective feedback which sustains the conveyor (as in Stommel's model of two adjacent boxes[16]), the new mechanism is due to a convective feedback (described in Welander's model of two vertically stacked boxes[17]), which makes convection partly a self-sustaining process. Lenderink and Haarsma[18] have recognised that this convective feedback leads to multiple steady states in three-dimensional circulation models, because some model grid points can have convection 'on' or 'off' under the same forcing, depending only on initial conditions. A large number of model equilibria with different convection patterns are therefore possible. With a realistic atmospheric heat budget like equation (1), the result is different climate states and the possibility of transitions between these states.

Figure 4 shows the convection patterns for the three different model equilibria. The transition between these states was in this case initiated when the freshwater inflow (at a rate of 0.32×10^6 m^3 s^{-1}) capped the high latitudes, effectively erasing

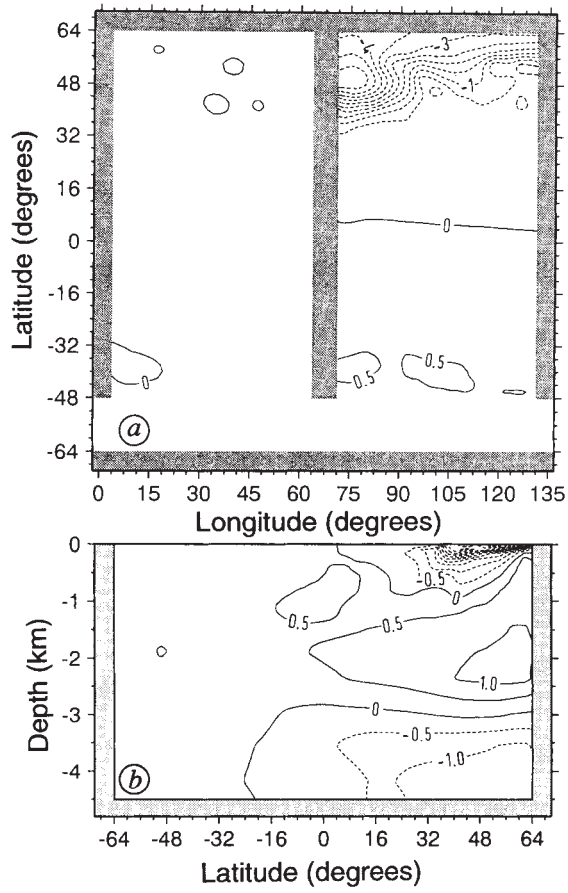

FIG. 3 Spatial structure of the temperature difference between warm and cold conveyor solution, shown in Fig. 1*a b*. Contour interval, 0.5 °C. *a*, Surface map. The maximum temperature drop is 5.3 °C in the western boundary current. *b*, Latitude–depth section along the western Atlantic basin. Cooling is concentrated near the surface in the North Atlantic, while the NADW outflow level warms. Some cooling occurs below 3 km depth due to the northward incursion of AABW.

the former convection pattern. More controlled transitions without blanket interruption of convection are also possible, using small 'surgical' freshwater perturbations targeted at single convection cells[15]. The actual meltwater release during the Younger Dryas event has been estimated as peaking at 0.44×10^6 m^3 s^{-1} (ref. 19).

A simple way of estimating the conveyor's heat transport is to multiply its mass transport by the temperature difference between warm inflow and cold deep outflow (see below). If this heat transport is large, the high latitudes are warm. But a large heat transport (given a fixed mass transport) requires cold outflow, seemingly at odds with warm high latitudes. This apparent contradiction is explained by the fact that convection can connect the deep outflow to the surface in different places, allowing its temperature to increase when the high latitude surface temperature drops. This is clearly seen in Fig. 3*b*. What has been dubbed a 'cold' conveyor (associated with cold sea surface temperature, SST) is thus one with a warm deep branch and reduced heat transport, due to relatively warm deep-water formation sites. Deep-water temperature and thus meridional heat transport seem to depend mainly on the latitude of convection; when convection moves south after the first perturbation the surface temperature drops, and when convection moves north after the second perturbation it increases again (see Fig. 4).

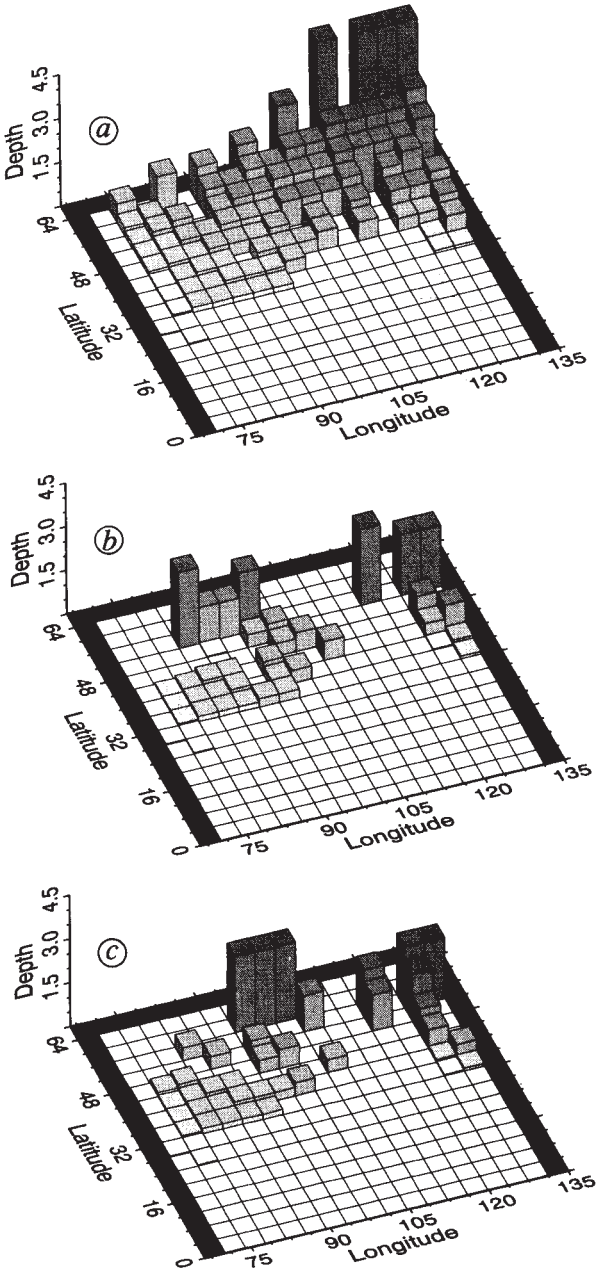

FIG. 4 Convection patterns in the North Atlantic basin, for the three equilibria shown in Fig. 1. The depth (km) of convection in each grid cell is plotted as a vertical bar. Shading is proportional to the number of model levels involved in convection.

The difference in oceanic heat transport between the warm conveyor (Fig. 1*a*) and the cold conveyor (Fig. 1*b*) peaks at 1.1×10^{14} W at 44° N, reducing the conveyor's heat transport across this latitude by 30%. In equilibrium this is balanced by a reduction in surface heat loss of 13 W m^{-2} averaged over the region north of 44° N. To achieve this heat flux change solely through longwave radiation (first term in equation (1)) would require an average SST change of 4.2 °C. The actual change in SST over this region is only 2.3 °C, demonstrating how part of the change in the conveyor's heat transport is compensated by a change in atmospheric transport (second term in equation (1)). The compensation by atmospheric transport is less effective for the change in heat budget than for the conveyor's budget as a whole, because the convective temperature changes are concentrated so far north. If the conveyor's heat transport is written as $c_p \rho m \Delta T$ (where c_p and ρ are heat capacity and density of sea water, m is the conveyor's mass transport of 13×10^6 m^3 s^{-1}, and ΔT is a characteristic temperature difference between warm northward- and cool southward-flowing branch), then a change in ΔT of 2 °C is sufficient to cause the heat transport change discussed above (compare this to Fig. 3*b*).

These multiple conveyor-belt states are similar to the ones found recently by Weaver and Hughes[20] and linked by these authors to rapid interglacial climate flunctuations. The crucial difference is that climate changes in their model are caused by changes in the conveyor's mass transport rather than its temperature. This model was driven with a traditional restoring boundary condition on SST, corresponding to fixed atmospheric temperature.

Are the climate transitions found in our model realistic? Preliminary results with a realistic topography global ocean model show similar multiple convection states (S.R., manuscript in preparation). Although 'pure' multiple equilibria under the same forcing would never arise in the real ocean under an ever-changing, 'noisy' atmosphere, the main conclusion of this model study remains valid: a shift in convection sites, whether it occurs through atmospheric changes, meltwater inflow or some other cause, could change the conveyor's heat transport and North Atlantic climate, even if deep-water formation continues at a similar rate.

A further question is whether present ocean climate models, which are hydrostatic and parametrize convection as a vertical mixing of statically unstable water, can represent deep-water formation in a realistic way. The crucial issue is whether convection events in nature act as 'mixing agents', causing vertical homogenization of the water column but practically no direct net sinking, or whether they act as a 'conduit' through which water is channelled downward to form new deep water. Send and Marshall[21] have recently shown that the former is true, justifying the approach taken in ocean circulation models.

Although our idealized model does not address this issue, it is tempting to speculate which regional shifts in convection sites might occur in the real ocean. Present NADW formation sites are the Norwegian Sea and Labrador Sea. Lehman and Keigwin[22] have suggested that the conveyor did not cease entirely during cold periods, but that only its lower branch, which originates in the Norwegian Sea, was interrupted. The model results presented here are consistent with this idea and give it an additional twist: they suggest that when deep-water formation is

reduced in the Norwegian Sea it may increase in the Labrador Sea, so that the two regions act like a see-saw. Climate cooling is then not caused by an overall weakening of the conveyor, but by a reduction in its heat transport related to the higher temperature of Labrador Sea convection.

These model experiments demonstrate that in order to explain rapid cooling events we need not invoke a total collapse of the conveyor; rather more subtle changes can cause a temperature drop in the northern North Atlantic of up to 5 °C. □

Received 16 June; accepted 23 September 1994.

1. Veum, T. *et al. Nature* **356,** 783–785 (1992).
2. Lehman, S. J. & Keigwin, L. D. *Nature* **356,** 757–762 (1992).
3. Zahn, R. *Nature* **356,** 744–746 (1992).
4. Boyle, E. A. & Keigwin, L. *Nature* **330,** 35–40 (1987).
5. Keigwin, L. D. *et al. J. geophys. Res.* **96,** 16811–16826 (1991).
6. Trenberth, K. E. & Solomon, A. *Clim. Dyn.* **10,** 107–134 (1994).
7. Levitus, S. *Climatological Atlas of the World Ocean* (US Dept of Commerce, NOAA, Washington DC, 1982).
8. Manabe, S. & Stouffer, R. J. *J. Clim.* **1,** 841–866 (1988).
9. Maier-Reimer, W. & Mikolajewicz, U. in *Oceanography* (eds Ayala-Castañares, A., Wooster, W. & Yáñez-Arancibia, A.) 87–100 (UNAM, México, 1989).
10. Marotzke, J. & Willebrand, J. *J. phys. Oceanogr.* **21,** 1372–1385 (1991).
11. Haney, R. L. *J. phys. Oceanogr.* **1,** 241–248 (1971).
12. Rahmstorf, S. & Willebrand, J. *J. phys. Oceanogr.* (in the press).
13. Sarnthein, M. *et al. Paleoceanography* **9,** 209–267 (1994).
14. Kushnir, Y. *J. Clim.* **7,** 142–157 (1994).
15. Rahmstorf, S. *J. Clim.* (in the press).
16. Stommel, H. *Tellus* **13,** 224–230 (1961).
17. Welander, P. *Dyn. Atmos. Oceans* **6,** 233–242 (1982).
18. Lenderink, G. & Haarsma, R. J. *J. phys. Oceanogr.* **24,** 1480–1493 (1994).
19. Fairbanks, R. G. *Nature* **342,** 637–642 (1989).
20. Weaver, A. J. & Hughes, T. M. C. *Nature* **367,** 447–450 (1994).
21. Send, U. & Marshall, J. *J. phys. Oceanogr.* (in the press).
22. Lehman, S. J. & Keigwin, L. D. *Nature* **358,** 197–198 (1992).

ACKNOWLEDGEMENTS. I thank J. Willebrand for assistance, R. Zahn, M. Rhein and E. Suess for discussions, and D. Smart for improving the clarity of the language in this Letter. This work was supported by the Deutsche Forschungsgemeinschaft; computations were performed at the German Climate Computer Centre in Hamburg.

Experimental simulations of explosive degassing of magma

H. M. Mader*, Y. Zhang†, J. C. Phillips‡, R. S. J. Sparks‡, B. Sturtevant§ & E. Stolper‖

* Institute of Environmental and Biological Sciences, Lancaster University, Lancaster LA1 4YQ, UK
† Department of Geological Sciences, University of Michigan, Ann Arbor, Michigan 48109–1063, USA
‡ Department of Geology, University of Bristol, Bristol BS8 1RJ, UK
§ Graduate Aeronautical Laboratories, ‖ Division of Geological and Planetary Sciences, California Institute of Technology, Pasadena, California 91125, USA

THE violent release of volatiles in explosive volcanic eruptions is known to cause fragmentation of magma and acceleration of the resulting mixture of gas and pyroclasts to velocities exceeding 100 m s^{-1} (ref. 1). But the mechanisms underlying bubble nucleation, flow acceleration and fragmentation are complex and poorly understood. To gain insight into these phenomena, we have simulated explosive eruptions using two model systems that generate expansion rates and flow velocities comparable to those observed in erupting volcanos. The key feature of both experiments is the generation of large supersaturations of carbon dioxide in a liquid phase, achieved either by decompressing CO_2-saturated water or by rapid mixing of concentrated K_2CO_3 and HCl solutions. We show that liberation of CO_2 from the aqueous phase is enhanced by violent acceleration of the mixture, which induces strong extensional strain in the developing foam. Fragmentation then occurs when the bubble density and expansion rate are such that the bubble walls rupture. In contrast to conventional models of fragmentation[1,2], we find that expansion and acceleration precede—and indeed cause—fragmentation.

The experiments were carried out (Fig. 1) at the University of Bristol and the California Institute of Technology using shock-tube techniques first proposed in this context by Bennett[3] and more recently developed in studies of volcanic jets[4], explosive vaporization[5] and high-speed dense dusty gases[6,7]. A crucial characteristic of the natural systems that we have tried to match in our experiments is that the volatile component (largely H_2O and/or CO_2 in real volcanic eruptions) is in a gaseous state after exsolution but the liquid component (in nature, a silicate liquid ± crystals), which makes up most of the mass of the system, is essentially entirely condensed, even after the volatile component has nearly completely exsolved. In these respects the systems in our experiments differ significantly from one-component systems[5] and two-component systems that completely (or nearly completely) evaporate on decompression.

Design of small-scale experiments to model large-scale volcanic phenomena requires consideration of scaling and dynamic similarity, but no scaling relationships have been established[8] for rapidly degassing bubbly liquids or the high-velocity high-density gas–particle flows that they generate[7]. Thus it is desirable to conduct simulations at the same velocity and with accelerations and flow densities similar to those in the large-scale setting. Velocities in our experiments approach those of volcanic flows (~100 m s^{-1})[1], as do the accelerations (~100g, ref. 7; note that gravity (1g) is unimportant in flows that experience such large accelerations). The high velocities and accelerations experienced by these flows mean that inertial rather than viscous forces control the dynamics. The ratio of the test-cell pressure to reservoir pressure in the decompression experiments (Fig. 1*a*) ranges from 30 to 300, comparable to magmas with a few per cent dissolved water (saturation pressures ~50–100 MPa) that disrupt explosively at a few megapascals (refs 2, 9). Obviously, the length scales of the volcanic system cannot be reproduced in the laboratory. Generally, in the study of bubbly liquids and dusty gases, the diameter of the laboratory flow channel is chosen to be much larger than the smallest bubble or particle class being modelled[7,10] so that the long-range dynamical interactions between phases that generate a variety of flow scales are free to act.

Bubble nucleation and growth are ultimately the processes that drive the accelerations observed in our experiments, so scaling of our results to nature requires an evaluation of how they may differ in supersaturated magmas. Molar fractions of volatiles in our experiments (up to 0.004 for CO_2 in the depressurization experiments, and as large as 0.1 in the chemical injection experiments) are comparable to those of intermediate to silicic magmas (0.02–0.06 for H_2O)[2], so the ratio of gas to condensed matter is comparable in the experiments and in nature. However, the diffusivity of CO_2 in H_2O (2×10^{-9} m^2 s^{-1} at 20 °C)[11] is ~200 times larger than that of H_2O (at concentrations of about 0.03) in magma at 850 °C (~10^{-11} m^2 s^{-1})[12,13]. The diffusively-controlled volume growth rate of bubbles during degassing is proportional to the product of diffusivity and concentration, which ranges from ~10 times larger than in magma in the decompression experiments to locally 200 times in the chemical experiments. The viscosity of water is also many orders of magnitude less than that of magma in explosive eruptions. But numerical calculations (ref. 14 and J. Barclay, D. S. Riley and R.S.J.S., unpublished results) indicate that, even under conditions of explosive eruption, diffusive bubble growth is not retarded by viscous effects unless magma viscosities exceed 10^8 Pa s. In the fragmentation region, with pressures of a few megapascals, magmas are not fully degassed and a few tenths of a per cent of residual dissolved water are sufficient to keep viscosities at values that would not inhibit explosive expansion